Rijksuniversiteit Groningen
KVI-CART & Medusa Radiometrics

Physics bachelor research project

Gamma ray Spectroscopy

Data merging for a multiple detector survey

Student:
J. Knijpstra (S3244571)

Supervisors:
Dr. E. van der Graaf
Dr. C. Rigollet
S. van der Veeke
Dr. J. Limburg

Abstract

Data is collected from several gamma ray detectors at the same time, however due to differences in efficiency, geometry and origin of the systems, these detectors do not produce identical data. In this research, the differences between distinct detectors are explored and it is investigated how to combine their signals and how measurements compare with theoretical predictions according to detector characteristics.

July 5, 2019

rijksuniversiteit
groningen

Contents

1 Introduction **2**

2 Theory **3**
2.1 Photonic interactions with matter . . . 3
2.1.1 The photoelectric effect . . . 3
2.1.2 Compton scattering . . . 3
2.1.3 Pair production . . . 3
2.1.4 Comparing the different interactions . . . 4
2.1.5 Attenuation . . . 4
2.2 Scintillation detectors . . . 5
2.3 The gamma ray spectrum . . . 6

3 Methodology **8**
3.1 Spectrum analysis and fitting methods . . . 8
3.1.1 The windows method . . . 8
3.1.2 Full spectrum analysis . . . 9
3.2 Double detector survey . . . 10
3.2.1 Setup . . . 10
3.2.2 Merging data . . . 10
3.3 Shielding . . . 11

4 Results **12**
4.1 Double detector survey . . . 12
4.1.1 Radionuclide concentrations . . . 12
4.1.2 Count rates . . . 14
4.2 Shielding experiment . . . 14
4.3 Scaled nuclide calibrations . . . 15

5 Discussion **19**

6 Conclusion **21**

7 References **22**

1 Introduction

Medusa Radiometrics BV develops spectrometer systems suitable for measuring gamma ray spectra of natural radioactive sources through which soil concentrations of radionuclides ^{40}K, ^{232}Th and ^{238}U and members of their decay series can be determined, although not all of these members necessarily decay through gamma emission. Spectra are recorded in histograms where the number of counts in each channel is measured during a certain live-time. In situ gamma-ray detectors usually use 256 or 512 channels, covering a range of about 100 keV to 3 MeV for radiation from terrestrial sources (from now on referred to as natural gamma radiation). Because radioactive decay is a stochastic process, it is important to collect enough data to reach a certain statistical (un)certainty. Relative uncertainties become smaller with a greater number of counts, so statistics are determined by source activity, live-time for each measured spectrum, and the efficiency of the scintillation-crystal, which in turn is highly dependent on the volume and density of the crystal. In this research, it is investigated how measured spectra from scintillation detectors with different characteristics can be combined and how their uncertainties should be propagated. Processing spectra from two detectors and adding these together should in theory produce equivalent results to first combining the two spectra and processing them afterwards, but this is not completely valid in practice, and it is investigated under what conditions the order of operations is interchangeable. In the next section, theory about interactions of gamma radiation with matter is presented. This is followed by a section on methodology in which spectrum analysis methods and experiment design are discussed. Following this is a section on experimental results and analysis, and finally a discussion and a conclusion section.

2 Theory

Ionising radiation exists in three forms: alpha-, beta-, and gamma radiation. Because alpha- and beta-radiation do not possess sufficient penetrative power to escape from soil and penetrate a scintillation crystal, only gamma radiation can be detected with Medusa's detector systems. These gamma rays are nothing but photons emitted at fixed energies in the decay of unstable isotopes. Although gamma rays have much greater penetrative power than alpha- and beta-radiation, they too can experience attenuation in a medium, and there is a multitude of different interactions they can undergo, which are explored in the following section.

2.1 Photonic interactions with matter

Unlike charged particles, photons do not lose energy proportionally to some distance travelled in a medium, but rather propagate freely until they undergo some form of interaction with the medium. At the energy scale of natural gammaradiation, the relevant interaction mechanisms are the photoelectric effect, Compton scattering, and pair production, which will be discussed in further detail in this section.

2.1.1 The photoelectric effect

In a photoelectric interaction, the energy of the incoming photon is fully absorbed by an atomic electron of the material it is penetrating, resulting in the ejection of the electron, in this context referred to as a photo-electron. The probability that will photon undergo this kind of interaction is expressed as a cross-section per unit mass (τ), which is (approximately) inversely proportional to the photon energy E_γ cubed and proportional to the atomic number Z to the power $n = 3 \sim 4$:[1]

$$\tau \propto Z^n E_\gamma^{-3} \tag{1}$$

2.1.2 Compton scattering

For the Compton effect, the energy of the incoming photon is only partially absorbed by an atomic electron, and the rest of the energy is carried away by a secondary photon. The Compton cross-section τ is more or less independent of the medium, and is inversely proportional to the photon energy:

$$\sigma \propto E_\gamma^{-1} \tag{2}$$

2.1.3 Pair production

In this interaction, a photon creates a particle in conjunction with its antiparticle:

$$\gamma \rightarrow e^- + e^+$$

The threshold energy for this interaction to occur is the sum of the rest masses of the created particles, which is 1.022 MeV for an electron-positron pair. Pair production becomes dominant at energies greater than 4 MeV. The interaction cross-section for pair production is denoted by κ and is described by an intricate

function of the energy and atomic number of the material that requires quantum field theory to calculate, but it generally scales with the square of the atomic number of the material $\kappa \propto Z^2$ and increases with the gamma ray energy E_γ.

2.1.4 Comparing the different interactions

In figure 1, the relative importance of each of the so far described photo-interactions can be seen as a function of E_γ and Z. The lines show for which atomic numbers Z and gamma energies $E_\gamma = h\nu$ the effects of the different interactions are equal in terms of interaction cross-sections[3]. Note that for natural gamma radiation, the energy range of 100 keV to about 3 MeV is considered, where pair production is never dominant.

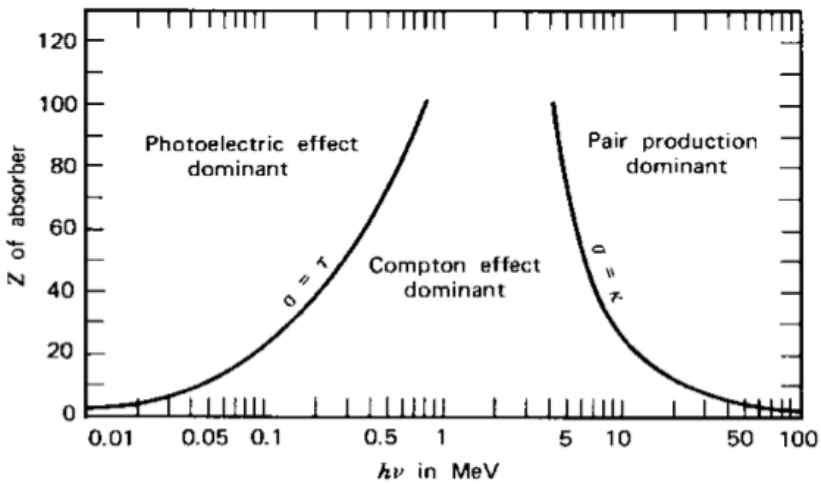

Figure 1: Dominant areas of the three discussed photo-interactions as a function of photon energy and atomic number of the absorbing material

2.1.5 Attenuation

A beam of photons travelling through a medium loses intensity because some of the photons will undergo interactions with the medium, such as the photoelectric effect, compton scattering or pair production. The probability per unit path length that a photon will be removed from the beam can be described by the linear attenuation coefficient μ, which is dependent on the energy of the photon and the density and effective atomic number of the medium. Since this coefficient describes the probability of a gamma ray undergoing any interaction, it can thus be expressed as the sum of the interaction cross-sections of the relevant (in this energy range) types of photo-interactions $\mu = \tau + \sigma + \kappa$. An approximately material-independent form is the mass-attenuation coefficient $\mu' = \mu/\rho$. The number of photons N in a mono-energetic beam (E_γ) that successfully traverse a homogeneous medium of thickness z without being removed from the beam

can be described by the following equation:

$$N(E_\gamma) = N_0 e^{-\mu E_\gamma z} \tag{3}$$

With N_0 being the initial number of photons in the beam. Attenuation is relevant when measuring radioactivity from soil, as the emitted radiation from these sources will be attenuated by the soil mixture and the air (especially in an airborne detector setup) that are above it. To approximate the attenuation caused by the different layers of such a mixture, it is possible to take the sum of the mass-attenuation coefficients of the different substances in each layer, weighted by their mass fractions in the mixture.

$$\mu'_{mixture} = \sum_i m_i \mu'_i$$

2.2 Scintillation detectors

Scintillation detectors consist mainly of a scintillation crystal and a photomultiplier tube. When gamma rays penetrate the crystal, they can undergo interactions with this scintillation material through for instance the Compton effect or the photoelectric effect and excite atoms in this medium. When the excited atoms de-excite, low-energy photons are emitted in quantities proportional to the energy of the radiation that caused the excitation. A photomultiplier tube then converts this scintillation light into an electrical signal. Through this process, we end up with a voltage proportional to the energy of the incident photon. See figure 2 for a schematic overview of a typical scintillation detector system[2].

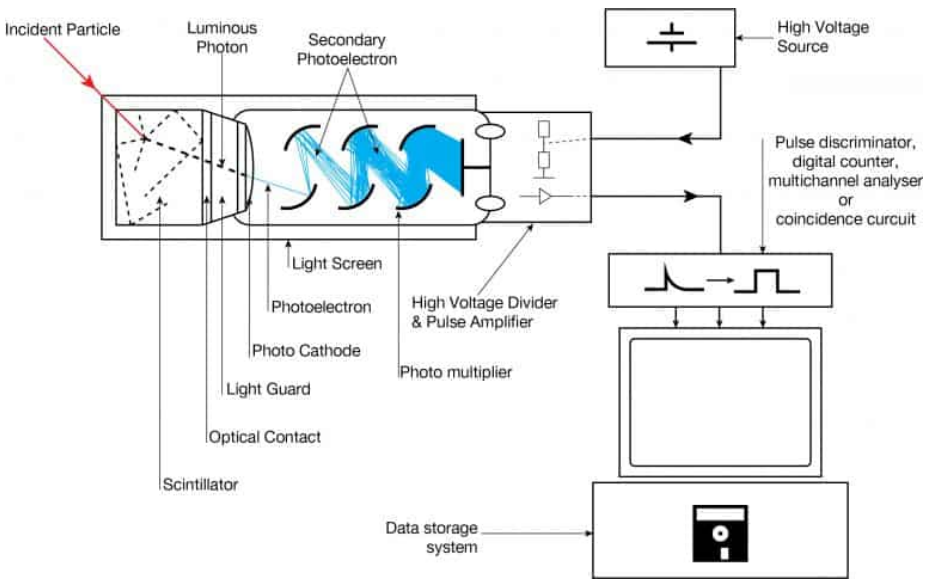

Figure 2: Schematic figure of a scintillation detector

Note that photons can also pass through the crystal without undergoing any kind of interaction, meaning they will not be detected, which becomes more likely at higher energies. Because of this, a crystal of greater volume will detect more counts than a small volume crystal. The density of the crystal is another important parameter that needs to be considered, as having a greater density will increase the probability of incoming radiation undergoing interactions.

MEDUSA develops inorganic scintillation detectors of different sizes and with different types of scintillation crystals, such as NaI and CsI. These all have intrinsic characteristics that should be considered when choosing a type of crystal to use in a detector. NaI is a very commonly used crystal because it is available in large volumes and has a moderate resolution. Because NaI is very brittle, it is preferable to use a less fragile type of crystal like CsI in some applications. The density of CsI is slightly higher and its resolution slightly worse than that of NaI. The disadvantage of using a CsI crystal lies mostly in its production cost, as it is about twice as expensive to produce as an NaI crystal of the same volume.

2.3 The gamma ray spectrum

A natural gamma ray spectrum is typically presented in a histogram, with energies ranging from 0 MeV to 3 MeV on the horizontal axis, and the number of counts registered for each energy channel during the measured time on the vertical axis. The shape of this spectrum is characterized by a number of energy 'peaks', which are due to gamma radiation always being emitted at specific energies. The relative heights of these peaks are dependent on the radioisotope composition of what is being measured; when measuring a source that is rich in potassium (i.e. has a high ^{40}K activity), for instance, the characteristic ^{40}K peak at 1460 keV will be relatively high. Besides the characteristic peaks of certain isotopes, the spectrum always includes a continuum due to Compton interactions of the incoming gamma rays with the detector. In figure 3[3], typical response curves for a CsI detector to radioisotopes ^{40}K, ^{238}U, and ^{232}Th are presented.

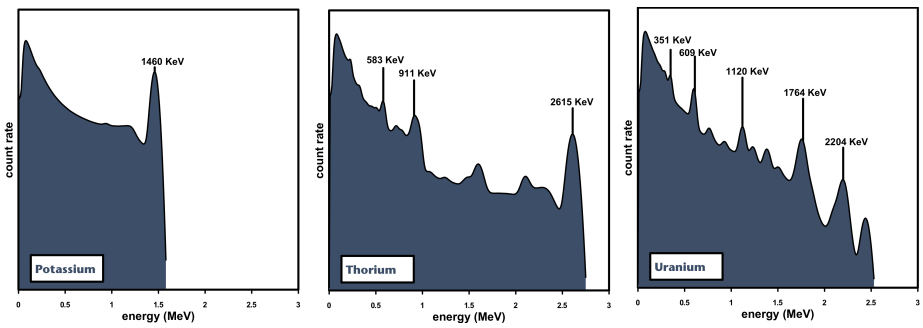

Figure 3: Gamma spectra of naturally occurring radioisotopes.

For each radioisotope, one or multiple peaks and a Compton continuum at the left of each peak can be observed. These curves can be interpreted as the so-called "standard spectra" of these nuclides, and are used in spectrum analysis.

An overview of the decay chains of ^{40}K, ^{238}U, and ^{232}Th is presented in figure 4, with the most relevant gamma ray emitters shown in grey boxes. From these decay chains, it becomes clear why ^{40}K has only one peak in its gamma spectrum, while ^{238}U and ^{232}Th have multiple peaks.
Sometimes ^{137}Cs is also included in the analysis, depending on whether it is present in the soil in question. Virtually all ^{137}Cs in Europe originates from nuclear fallout from the Chernobyl disaster in 1986, but it did not reach all areas, so whether the presence of ^{137}Cs is significant enough to be included in gamma spectrum analysis depends on the location.

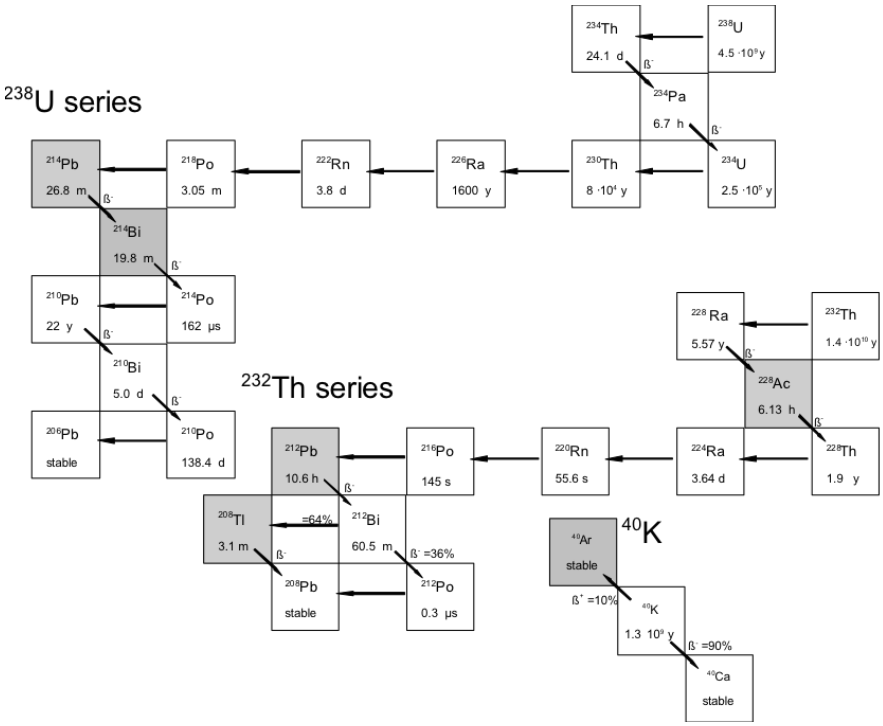

Figure 4: Decay chains of naturally occurring radioisotopes

3 Methodology

3.1 Spectrum analysis and fitting methods

A gamma ray spectrum obtained when measuring a soil will be some linear combination of the standard spectra. If the expected shapes of the spectra of the individual nuclides are known (standard spectra), activity concentrations of these nuclides can be inferred from their combined spectra. These standard spectra can be generated with so-called Monte-Carlo simulations, where the decay (a stochastic process) at a concentration of 1 Bq kg^{-1} of a certain radioisotope is simulated for the desired detector geometry. In addition, a calibration file specific to the detector is required to calibrate the data and make sure that each peak is in the expected channel. This is achieved with the FSA method described later in this section. Every detector is to some degree unique and needs to be characterised separately in a well-defined (with respect to radionuclide concentrations and geometry) calibration environment such as the *stonehedge* facility at Medusa.[4]

There exist two commonly used approaches in analysing gamma spectra. One such method is known as windows analysis, in which nuclide concentrations are determined by considering the area under individual peaks. A more recently developed alternative is called full-spectrum analysis (FSA), in which the entire spectrum shape is taken into account and is separated into a background and a linear combination of standard spectra.[5]

3.1.1 The windows method

In windows analysis, one starts by finding a scaling parameter for the counts in the "window" of the main thorium peak. This peak happens to occur at an energy (2615 keV) where the other nuclides contribute virtually nothing to the spectrum (see figure 3 or 5), and one thus straightforwardly solves one equation with one unknown parameter. One can then apply the same method to the main uranium peak, where some counts due to thorium need to be subtracted first, but then reduces to another equation with one unknown. Also applying this to ^{40}K, the entire fitting procedure reduces to solving the set of equations:[6]

$$C_{\mathrm{K}} = (n_{\mathrm{K}} - \beta n_{\mathrm{Th}} - \gamma(n_{\mathrm{U}} - \alpha n_{\mathrm{Th}}))/s_{\mathrm{K}} \tag{4}$$

$$C_{\mathrm{U}} = (n_{\mathrm{U}} - \alpha n_{\mathrm{Th}})/s_{\mathrm{U}} \tag{5}$$

$$C_{\mathrm{Th}} = n_{\mathrm{Th}}/s_{\mathrm{Th}} \tag{6}$$

Here, the counts in the windows of each nuclide are denoted by n_{K},n_{U}, and n_{Th}, with the contents corrected for the specific detector and for a cosmic background. The factors s_i represent the detection sensitivities in each windows. The factors α, β and γ are corrections for Compton contributions of photopeaks at higher energies to lower energy windows, known as stripping factors.[5]. A problem with this method is that the background subtraction introduces great uncertainties, especially when dealing with low activities.[6]

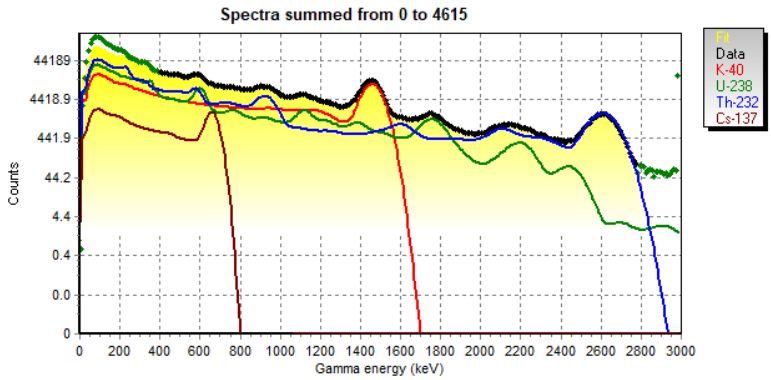

Figure 5: Typical FSA fitted spectrum

3.1.2 Full spectrum analysis

Compared to windows analysis, FSA is a computationally more intensive endeavour, as there are many more parameters that need to be simultaneously optimsised. The measured spectrum Y is described as a sum of the standard spectra X_j multiplied by the activity concentrations C_j for the individual nuclides, plus a background spectrum (BG). The optimal activity concentrations can be found using a least-squares method:[5]

$$\chi^2 = \frac{1}{N-M} \sum_{i=1}^{N} [Y(i) - \sum_j C_j X_j(i) - BG(i)]^2 / w(i) \tag{7}$$

In this equation, i is the channel number and goes up to N, $w(i)$ is a weight factor and M is the number of standard spectra. By analysing the full energy spectrum, the derived concentrations are less sensitive to spectrum drift compared to those calculated using an exactly determined set of equations in the windows approach. Additionally, the contribution of gamma rays that do not fall into any of the windows also makes for an overall higher quality fit with the FSA approach.[5]

3.2 Double detector survey

3.2.1 Setup

A gamma detector survey was carried out with two detectors of different geometries. The two detectors used were mounted on the back of an ATV (quad-bike). The ATV was driven in lines separated by approximately 10 meters over a field near the city of Ghent, Belgium, while the two detectors were simultaneously collecting data. The first detector used was the MS2000 (left in figure 6) with a 2 litre CsI crystal, and the other was an MS1000 detector (right in figure 6) with a 1 litre CsI crystal.[7]

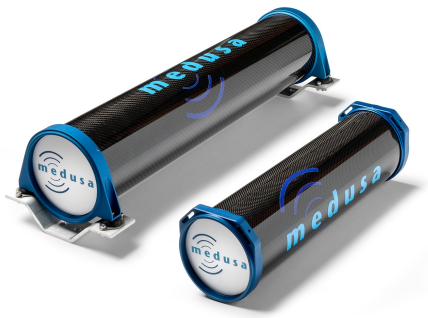

Figure 6: "Ms2000" and "MS1000" detectors

The two data sets produced by the two detectors were processed separately using Medusa's analysis toolbox named Gamman. For both data sets, five spectra measured at a frequency of 1 Hz were merged into one spectrum and were fitted using FSA, leaving us with five times fewer spectra, but each with better counting statistics.

3.2.2 Merging data

Theoretically speaking, there is no difference between summing two spectra and then applying FSA to them, and first applying FSA to the spectra and then combining them. This latter approach was carried out by means of taking the weighted average of the average nuclide concentrations produced by the two detectors and adding their count rates. For the former approach, a method was developed to add two fitted spectra together using Python. Importing the data sets as csv-files, the spectra were separated from the other data (timestamps, gps data, real/live times, total counts, stabilisation parameters). Before adding the spectra, they first had to be synchronised, as the detectors were not turned on simultaneously. This was done by coupling the time stamps of both detectors that were closest to each other and shifting one of the two spectra to match the time stamps most closely. Variations in live time are small compared to the interval between each data point (5s) so only one pair of time stamps needed to be matched (and then a number of data points must be deleted to match data array dimensions). After having synchronised the two data sets, they were imported into Python as (numpy) arrays, added together, and exported

as another csv-file, which was to again be processed with Gamman in the same way as the data sets of the individual detectors, but using a new calibration file. All calibration files used were generated with simulations of a flatbed geometry (a flat surface with certain nuclide concentrations) with a detector at a height of 80 cm above the ground.

3.3 Shielding

From the data from the double detector survey, it was observed that concentrations measured with one detector were systematically higher than those measured with the other detector, and this was hypothesized to be due to a shielding effect (see results and discussion sections). To test this hypothesis, a second experiment was designed where the detectors were mounted on the ATV in the same way as they were while conducting the original survey, and statically measuring at one point on a homogeneous field. Additionally, data would be collected from both detectors at this point separately, at the same height above the ground, but without the ATV or the other detector to shield them.

The smallest difference in concentrations between the two detectors obtained in the original experiment was $(4.22 \pm 0.12)\%$ (see results section). To be certain of having sufficiently good statistics, it was chosen to aim for a 0.5% accuracy. Assuming Poisson statistics holds, and thus taking the square root of the number counts as our uncertainty, we can calculate a minimum measurement time needed to achieve our desired accuracy. From data acquired with the MS2000 on this same field, we know that for ^{40}K there was a recorded 0.272 counts per second for 1 Bq/kg, and an average concentration of 240.747 Bq/kg, implying a count rate of 65.48 counts/s. To find the required measurement time T to get a 0.5% uncertainty in our ^{40}K counts, we solve the equation

$$\frac{\sqrt{T_{40\mathrm{K}} * 65.48 s^{-1}}}{T_{40\mathrm{K}} * 65.48 s^{-1}} = 0.005 \tag{8}$$

Which has a solution of 611 s for ^{40}K. Applying this to the other nuclides results in a required measuring time of 664 s for ^{238}U and 524 s for ^{232}Th. This means we need to measure for at least $664s/60 \approx 11$ minutes for the MS2000. Count rates were about 56% higher in the MS2000 compared to the MS1000 in the original experiment with this configuration, so for measurements with the MS1000, a measurement time of about 17 minutes is required to obtain the same accuracy in counts.

Three separate measurements were carried out: one with both detectors gathering data simultaneously mounted on the ATV for 17 minutes, one for the MS1000 separately without the ATV and minimal shielding from the frame to which it was mounted for 17 minutes, and one measurement with the MS2000 mounted in the same way with minimal shielding, for 11 minutes. During these last two measurements, the detectors in question were mounted to a frame as is shown in figure 7, where the ATV was kept at a distance of a few meters to supply power. Shielding due to the ATV is assumed to be negligible at this distance.

Figure 7: MS1000 measurement setup with minimal shielding

4 Results

4.1 Double detector survey

To get an idea of what the measured field looks like, see figures 4.1 for a raw and an interpolated ^{40}K map of the measured field.

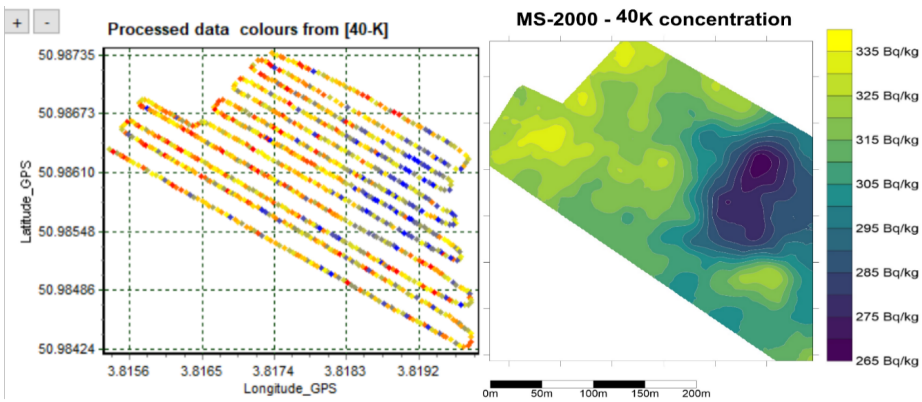

Figure 8: Left: Measured ^{40}K concentrations of field (1 point = 5 added spectra), blue and red colours indicate low and high concentrations respectively (244 to 375 Bq/kg) Right: ^{40}K map of field after interpolation

4.1.1 Radionuclide concentrations

See the following figure for the obtained radionuclide concentrations presented in a bar chart.

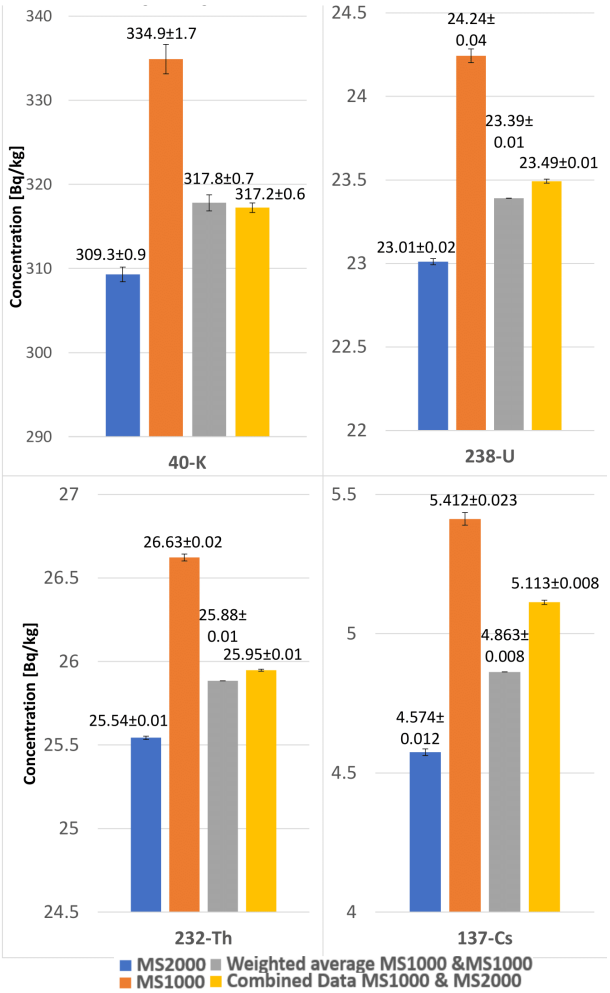

Figure 9: Average nuclide concentration comparison for combined and separate data

Comparing the 'combined' data with the separate data, it was observed that the averages of the inferred values for radionuclide concentrations of the combined data tend to be somewhere in between that of the MS1000 and the MS2000, but with alower uncertainty, and tend to be close to but slightly higher than the weighted averages of the MS1000 and the MS2000 (except in the case of ^{40}K where the uncertainties overlap). More surprisingly, it turns out that the average calculated concentrations are higher for the MS1000 data compared to the MS2000 data by (8.28±0.85)% for ^{40}K, (5.36±0.26)% for ^{238}U, (4.22±0.12)% for ^{232}Th, and $(18.3 \pm 0.76)\%$ for ^{137}Cs.

4.1.2 Count rates

In addition to the different nuclide concentrations measured by the two detectors, the count rates of both detectors were considered. The count rate of each detector is the number of registered counts per second after spectrum analysis. A detector with a greater crystal volume will of course register more counts per unit time than one with a smaller volume. It is observed that the MS2000 detects about 1.55 times as many counts per unit time than the MS1000 does in this configuration. When comparing the calculated count rates of the combined data and the data of the two separate detectors (not included in the figure above), one would expect the count rates of the combined data to be equal to the sum of the count rates of the two separate data sets. It turns out however, that the count rates from the combined data are systematically about three to five percent lower than these summed count rates.

4.2 Shielding experiment

In figure 10 a comparison is shown of nuclide concentrations and count rates measured by the MS1000 and MS2000 mounted on the ATV (blue and red), and these two detectors separately with minimal shielding. The same two 80 cm flatbed calibration files (one for each detector) were used as in the original experiment in Belgium, except ^{137}Cs was not included in this calibration and analysis, as there seemed to be no significant presence of this nuclide in the soil of this field. Just as in the original measurements, the concentrations measured by the ATV-mounted MS2000 turn out lower than those of the ATV-mounted MS1000. However, it is observed that the measured nuclide concentrations do not just differ between the two detectors mounted onto the ATV, but there are also differences between the ^{40}K and ^{232}Th concentrations as measured by both detectors separately without shielding that exceed uncertainties.

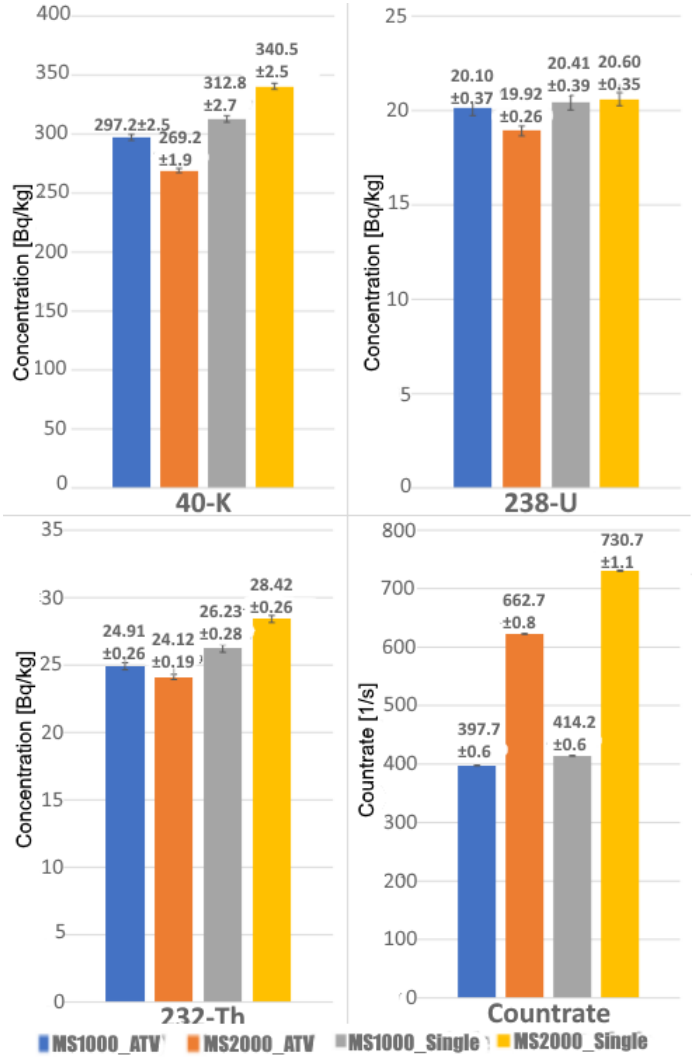

Figure 10: Nuclide concentrations and count rate comparison of the two detectors in both the ATV-mounted and separate configurations

4.3 Scaled nuclide calibrations

Both detectors are calibrated relative to the known concentrations of the bricks in the Stonehedge calibration facility, but with an uncertainty. Upon inspection of the calibration files of both detectors, it was found that the MS2000 was calibrated to scale up measured nuclide concentrations by greater factors than the MS1000. By then scaling down these nuclide concentrations in a new MS2000 calibration file to match those of the MS1000 calibration file, and using this to re-calibrate the MS2000 spectra, the results shown in figure 11 were obtained. It was found that the nuclide concentrations produced by the single measurements (without shielding) of both detectors, became much more similar with the errors

overlapping each other. At the same time, also having applied this newly made calibration file to the MS2000 data from the double (ATV) measurement, it was found that the MS2000 still produced significantly lower nuclide concentrations than the MS1000 did in this configuration. This tells us that the difference between the nuclide concentrations measured by the two detectors in the ATV-mounted configuration are not just due to an inherent difference in calibration of the detectors, but rather due to external effects like shielding. The data from

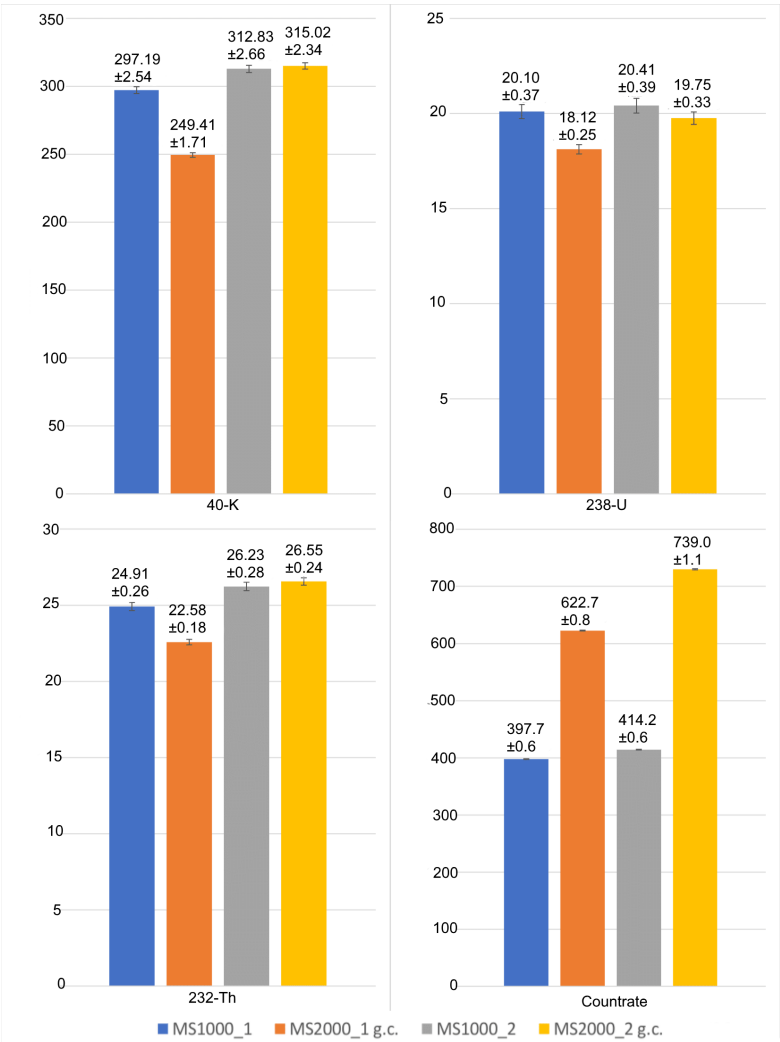

Figure 11: Concentrations and countrates from the shielding experiment, but with the MS2000 calibration scaled to MS1000 values. 1 and 2 indicate the mounted and separate configurations, respectively. "g.c." indicates the calibration file used had scaled down nuclide concentrations.

the MS1000 and MS2000 (with scaled-down calibration) in ATV-mounted configuration were also again 'combined' (=summing the spectra and reprocessing

them), where the concentration values were found to be in between those of the two separate detectors, as shown in figure 13. In order to combine the data, the summed spectra were processed with a newly produced calibration file. This calibration file was made by summing the spectra in the calibration file that was used for the MS1000, and the calibration file used for the MS2000 where nuclide concentrations were scaled down to match that of the MS1000 calibration. The count rate of the combined data was found to be $\mathrm{Cts}_{\mathrm{combined}} = 993.96 \pm 1.00$, while the sum of the separate count rates of the two ATV-mounted detectors was found to be $\mathrm{Cts}_{\mathrm{summed}} = 1020.4 \pm 1.0$.

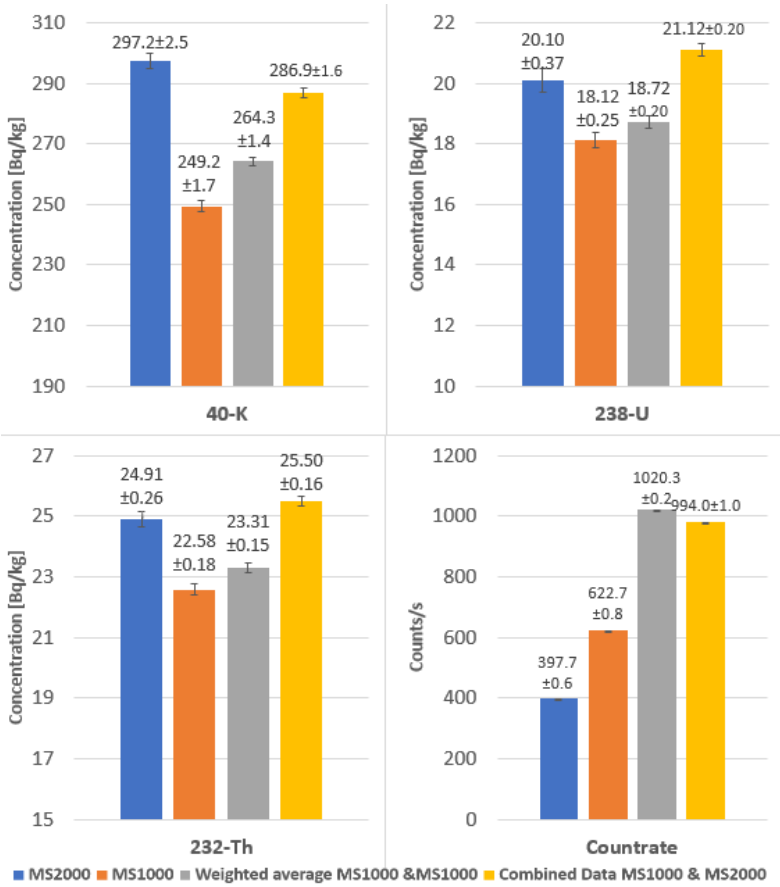

Figure 12: Comparing 'combined' data of the shielded MS1000 & MS2000 with the weighted averages of the separately obtained nuclide concentrations and the sum of their count rates.

Finally, the data sets from the two detectors in the single (no shielding) configuration were combined, also with the new calibration file. This resulted in concentrations higher than that obtained from both separate data sets, and a count rate that is lower than the sum of the two count rates from the seperate detectors ($(1117.8 \pm 1.3)\mathrm{s}^{-1}$ vs $(1144.2 \pm 1.2)\mathrm{s}^{-1}$). See the figure below.

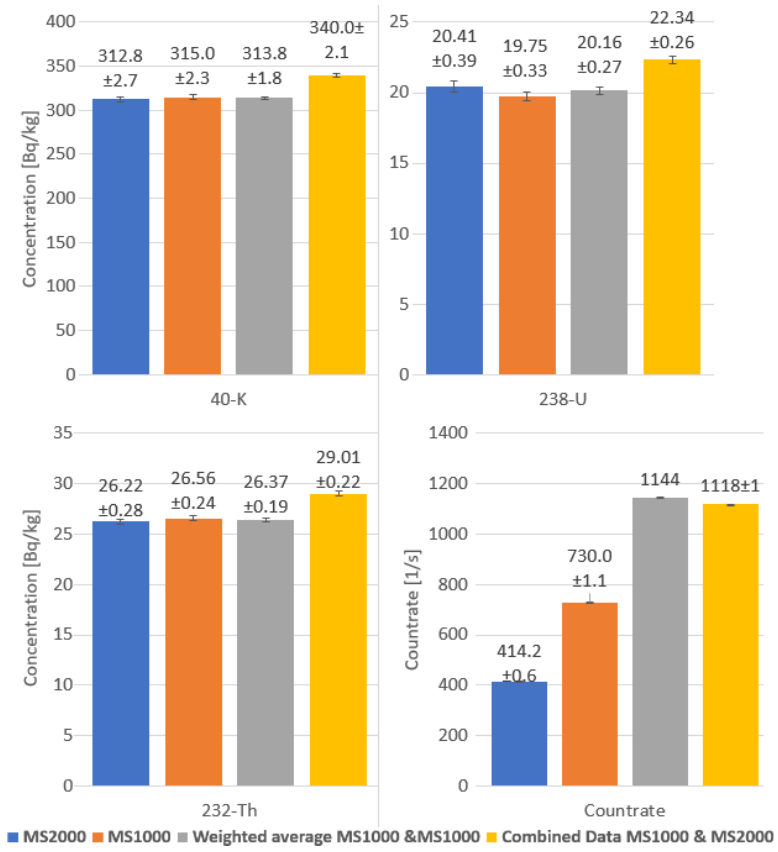

Figure 13: Comparing 'combined' data of the non-shielded MS1000 & MS2000 with the weighted averages of the separately obtained nuclide concentrations and the sum of their count rates.

5 Discussion

Since the MS2000 measurements were found to consistently result in lower nuclide concentrations than the MS1000 (see results section and figure 9), it was conjectured that shielding by the ATV and MS1000 could be of substantial influence to the MS2000 data, as the MS2000 detector was situated in between the ATV and the MS1000 detector. These lower calculated values for nuclide concentrations were especially pronounced for lower energy nuclides like ^{40}K, which could be explained by the fact that higher energy radiation has more penetrative power than lower energy radiation, and so some of the higher energy radiation was still able to penetrate the ATV and MS1000 without undergoing any interactions, while lower energy radiation is more likely to be detected by the MS1000 or to be absorbed by the ATV. See the figure below for a sketch of the mounted detector setup, with the lines indicating the areas where shielding could be of influence on the measurements. This implies that there exists some intrinsic difference in the way the two detectors collect their data.

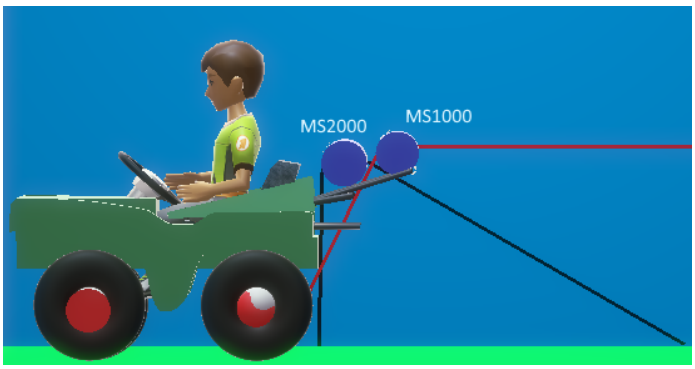

Figure 14: Schematic model of shielding situation on ATV

It was unexpected that the two detectors would yield different concentrations and count rates, even when they measured independently at the same location without significant shielding (see section 4.2 and figure 10). The argument that shielding is the cause of the unexpected difference is fortified by the fact that the concentrations obtained by the un-shielded measurements were higher for both detectors compared to their shielded counterparts, with the difference between the shielded and un-shielded MS2000 being greater than the difference between the two configurations of the MS1000 — suggesting the MS2000 experiences more shielding, as would be expected considering the geometry of the shielded configuration. As mentioned in section 4.3, the MS2000 registered higher radionuclide concentrations in the calibration used to process measured spectra. By manually scaling these concentrations down, a new calibration file was created, and was used to obtain the results shown in figure 11. In contrast to the previous results, these results showed no difference between the separately employed detectors in terms of nuclide concentrations, but still show lower concentrations for the MS2000 in the shielded configuration. This implied that the two detectors can in principle produce identical data, but that shielding is mitigating the flux through both detectors, though mainly the MS2000.

When combining the data of the shielded detectors in the same fashion as done originally with the data from Ghent (section 3.2.2), but with a new calibration file for the summed spectra, results similar to those in figure 9 were obtained; the concentrations obtained through the combined data were higher than the (weighted) averages of the concentrations from the separate detectors, but a count rate lower than the sum of the count rates of the two separate detectors (see figure 13). What was unexpected however, is that when combining the data from the two un-shielded detectors, concentrations and count rates different from the two separate detectors were obtained. These results were unexpected because it was thought that since shielding is assumed to be negligible, only innate differences between the detectors could cause flaws in the combined data, and innate differences were supposed to be mended by re-calibrating the MS2000. The reason for this unexpected result needs to be further investigated. It could be due to unjustified assumptions used to create the scaled calibration file for combining the two data sets.

6 Conclusion

From the measurements and analysis carried out in this report, it can be concluded that spectra from multiple detectors cannot be straightforwardly combined by adding their fitted spectra and reapplying full spectrum analysis. When this was attempted, concentrations and count rates of this combined data were not what would be expected when considering the data from the two separate detectors. In fact, it was even found that there were differences in the concentrations obtained by the two detectors separately, already before applying any new methods. This difference was attributed to be due to the effect of "shielding" in the measurement setup, and a new experiment was designed to test whether or not shielding was causing this discrepancy. From this experiment, it was concluded that shielding was likely to be influencing the results, but it was also observed that there was also a disparity between the detectors in a non-shielded setup. This disparity was corrected for by re-calibrating one of the detectors, and resulted in concentrations that were the same (within one sigma) in a non-shielding setup, but with a difference between the two detectors in a shielded setup. Finally it was again attempted to combine two data sets, this time of two detectors in a non-shielded configuration and with another new calibration file to adjust for the one detector being re-calibrated, but this resulted in concentrations that were too high, and an average count rate that was too low. Merging this data needs to be investigated further.

7 References

[1] James E. Turner (2007). Atoms, Radiation, and Radiation Protection. Chapters 3, 4, 8, 10.3.
ISBN 978-3-527-40606-7

[2] https://www.nuclear-power.net/nuclear-engineering/radiation-detection/scintillation-counter-scintillation-detector

[3] The medusa institute wiki https://the.medusa.institute/

[4] E.R. van der Graaf et al. (January 2011), Monte Carlo based calibration of scintillation detectors for laboratory and in situ gamma ray measurements. Journal of Environmental Radioactivity Volume 102, Issue 3, March 2011, Pages 270-282

[5] P.H.G.M. Hendriks et al (2000)., Full-spectrum analysis of natural γ-ray spectra. Journal of Environmental Radioactivity 53 (2001) 365–380

[6] Desbarats, A. J., Killeen, P. G. (1990). A least-squares inversion approach to stripping in gamma-ray spectral logging. Nuclear Geophysics, 4(3), 343–352.

[7] Medusa product information website https://the.medusa.institute/pages/viewpage.action?pageId=329290